

Proton fragmentation functions considering finite-mass corrections

S. M. Moosavi Nejad^{a,b,*}, M. Soleymaninia^{c,†} and A. Maktoubian^a

^(a) *Faculty of Physics, Yazd University, P.O.Box 89195-741, Yazd, Iran*

^(b) *School of Particles and Accelerators, Institute for Research in Fundamental Sciences (IPM), P.O.Box 19395-5531, Tehran, Iran*

^(c) *Department of Physics, Payame Noor University, P.O.Box 19395-3697, Tehran, Iran*

(Dated: November 11, 2018)

We present new sets of proton fragmentation functions (FFs) describing the production of protons from the gluon and each of the quarks, obtained by a global fit to all relevant data sets of single-inclusive electron-positron annihilation. Specifically, we determine their uncertainties using the Gaussian method for error estimation. Our analysis is in good agreement with the e^+e^- annihilation data. We also include finite-mass effects of the proton in our calculations, a topic with very little attention paid to in the literatures. Proton mass effects turn out to be appreciable for gluon and light quark FFs. The inclusion of finite-mass effects tends to improve the overall description of the data by reducing the minimized χ^2 values significantly. As an application, we apply the extracted FFs to make predictions for the scaled-energy distribution of protons inclusively produced in top quark decays at next-to-leading order, relying on the universality and scaling violations of FFs.

PACS numbers: 13.87.Fh, 13.66.Bc, 13.60.Hb, 13.85.Ni

I. INTRODUCTION

Fragmentation functions $D_i^H(z, \mu_F^2)$, describe the probability for a parton i at the factorization scale μ_F to fragment into a hadron H carrying away a fraction z of its momentum. They are key quantities for calculating hadroproduction cross sections. In this respect, one needs to determine these functions with high accuracy. Recently, in [1] pion fragmentation functions (FFs) are studied at next-to-next-to-leading order (NNLO) using data from e^+e^- annihilation.

The specific importance of FFs is due to their model-independent predictions of cross sections at the Large Hadron Collider (LHC). Specially, to study the properties of top quarks at the LHC, one of the proposed channels is to consider the energy spectrum of outgoing hadrons H from top decays in the process $t \rightarrow W^+b(\rightarrow H)$. For this purpose, having parton-level differential decay rates for the subprocess $t \rightarrow bW(g)$ at NLO [2–4] and FFs of partons into hadrons D_i^H ($i=b,g$), one can calculate the energy distribution of observed hadrons. For example, the CMS collaboration reconstructs the top mass from the peak of the energy distribution of bottom-flavored hadrons [5, 6]. Since the hadronization mechanism is universal and independent of the perturbative processes which produce the partons one can exploit, for example, the existing data on $e^+e^- \rightarrow b\bar{b} \rightarrow H + jets$ events to fit the proposed models for the FFs describing $b \rightarrow H$, and use them to make predictions for other processes, such as top decays $t \rightarrow W^+(\rightarrow l^+\nu_l) + b(\rightarrow H)$. FFs are also useful for theoretical calculations of inclusive hadron production at the Relativistic Heavy Ion Collider (RHIC)

and for investigating the origin of the proton spin.

Generally, there are two main approaches to evaluate the FFs. The first approach is based on the fact that the FFs for hadrons containing a heavy quark or anti-quark can be computed theoretically using perturbative QCD (pQCD) [7, 8]. The first theoretical attempt to explain the procedure of hadron production from a heavy quark was made by Bjorken [9] by using a naive quark-parton model. He deduced that the inclusive distribution of heavy hadrons should peak almost at $z = 1$, where z refers to the scaled-energy variable of hadrons. The pQCD framework was applied by Peterson [10], Suzuki [11], Amiri and Ji [12], while in this framework Suzuki calculates the heavy FFs by using a convenient Feynman diagram and considering a typical wave function for the hadronic bound states. One of us, using Suzuki's approach, has calculated the FFs for a charm quark to split into S-wave D^0/D^+ mesons [13] and for a gluon to split into S-wave charmonium states ($\eta_c, J/\psi$) [14] at leading order in the QCD coupling constant α_s .

In the second approach which is frequently used to obtain the FFs, these functions are parametrized in a specific model and extracted from experimental data analysis using the data from e^+e^- reactions, lepton-hadron and hadron-hadron scattering processes. This situation is very similar to the determination of the parton distribution functions (PDFs)[15]. Among all scattering processes, the best processes which provide a clean environment to determine the FFs are e^+e^- annihilation processes. However, without an initial hadron state one can not separate quark distributions from antiquark distributions. There are several theoretical studies on QCD analysis of FFs which used special parameterizations and different experimental data in their global analysis. Recent extracted FFs for light hadrons are related to AKK [16], SKMA [17, 18], LSS [19], DSEHS [20], DSS [21, 22] and HKNS [23] collaborations who used different phe-

*Electronic address: mmoosavi@yazd.ac.ir

†Electronic address: maryam_soleymaninia@ipm.ir

nomenological models and varying experimental data. In [17, 18], we determined the π^\pm and K^\pm FFs, both at leading order (LO) and NLO through a global fit to the single-inclusive e^+e^- annihilation (SIA) data and the semi-inclusive deep inelastic scattering (SIDIS) asymmetry data from HERMES and COMPASS. There, we broke the symmetry assumption between the quark and anti-quark FFs for favored partons by using the asymmetry data.

In this paper, we present a new functional form of proton FFs up to NLO, obtained through a global fit to SIA data from LEP (ALEPH and DELPHI collaborations), SLAC (SLD and TPC collaborations) and DESY (TASSO collaboration) [24–29]. We also impose the effects of the proton mass on the FFs, a topic with very little attention paid to in the literatures, e.g. [17–23]. We show that this effect is important in calculating gluon and light quark FFs, specifically at low energies. This effect reduces the minimized χ^2 and makes a more convenient fit.

In the Standard Model (SM) of particle physics the top quark has a short lifetime ($\tau_t \approx 0.5 \times 10^{-24} s$ [30]), so it decays before hadronization takes place. Therefore its full polarization content is retained when it decays. As was mentioned, one way to study its properties is to consider the energy distributions of the produced hadrons in top decays. Here, we also make predictions for the scaled-energy distribution of protons inclusively produced in top quark decays, $t \rightarrow W^+ + b(\rightarrow p + X)$, using the extracted FFs at our analysis and the parton-level Wilson coefficients calculated in [3, 4]. These predictions will also enable us to deepen our understanding of the nonperturbative aspects of proton formation by hadronization and to pin down the proton FFs.

This paper is organized as follows. In section II we describe the formalism and our parametrization of proton fragmentation functions at LO and NLO. Using the SIA data we present our fit results and shall compare our results against FFs from other well-known collaborations. We also describe the Gaussian method to calculate errors in our analysis. In section III, we explain how to impose the effect of the hadron mass on the FFs and compare our results in both cases. Our predictions for the energy spectrum of protons produced in unpolarized top quark decays are presented in section IV. Our results are summarized in section V.

II. QCD ANALYSIS OF PROTON FRAGMENTATION FUNCTIONS

A. Formalism

FFs are nonperturbative functions describing the hadronization processes, so they have an important role in the calculation of single-inclusive hadron production in any reaction. According to the factorization theorem of the parton model [31], the leading twist component of inclusive production measurement of any single hadron

can be written as the convolution of perturbative partonic cross sections, with nonperturbative FFs and PDFs to account for any hadrons in the initial and final states, respectively. As an example, the cross section for the production of hadron H in the typical scattering process $A + B \rightarrow H + X$, can be expressed as [32]

$$d\sigma = \sum_{a,b,c} \int_0^1 dx_a \int_0^1 dx_b \int_0^1 dz f_{a/A}(x_a, Q^2) f_{b/B}(x_b, Q^2) \times d\hat{\sigma}(a + b \rightarrow c + X) D_c^H(z, Q^2), \quad (1)$$

where a and b are incident partons in the colliding initial hadrons A and B , respectively, $f_{a/A}$ and $f_{b/B}$ are the PDFs at the scale Q^2 of the partonic subprocess $a + b \rightarrow c + X$, c is the fragmenting parton (either a gluon or a quark) and X stands for the unobserved jets. Here, $D_c^H(z, Q^2)$ is the FF at the scale Q^2 which can be obtained by evolving from the initial FF $D_c^H(z, Q_0^2)$ using the Dokshitzer-Gribov-Lipatov-Altarelli-Parisi (DGLAP) renormalization group equations [33].

Since we determine the FFs from single-inclusive hadron production data in e^+e^- annihilation, we do not need to deal with uncertainties induced by PDFs as in hadron collisions. The cross section for the single-inclusive e^+e^- annihilation processes, $e^+e^- \rightarrow (\gamma, Z) \rightarrow H + X$, is expressed as follows [31]

$$\frac{1}{\sigma_{tot}} \frac{d}{dx_H} \sigma(e^+e^- \rightarrow HX) = \sum_i \int_{x_H}^1 \frac{dx_i}{x_i} D_i^H\left(\frac{x_H}{x_i}, \mu_F^2\right) \frac{1}{\sigma_{tot}} \frac{d\hat{\sigma}_i}{dx_i}(x_i, \mu_R^2, \mu_F^2), \quad (2)$$

where, σ_{tot} is the total partonic cross section at NLO [34] and D_i^H indicates the probability to find the hadron H generated from a parton $i(=g, u/\bar{u}, d/\bar{d}, \dots)$ with the scaled-energy fraction $x_H = 2E_H/\sqrt{s}$ so that $s = q^2$ stands for the squared of the four-momenta of the intermediate gauge bosons γ and Z . In (2), x_i is also defined in analogy to x_H as $x_i = 2E_i/\sqrt{s}$ and the $d\hat{\sigma}_i/dx_i$ are the differential cross sections at the parton level for the $i\bar{i}$ pair-creation subprocesses; $e^+e^- \rightarrow (\gamma, Z) \rightarrow i\bar{i} + (g)$, which can be calculated in perturbative QCD [35–37]. In the equation above, μ_R and μ_F stand for the renormalization and factorization scales respectively, so one can use two different values for these scales; however, a choice often made consists of setting $\mu_F^2 = \mu_R^2 = Q^2$ and we shall adopt this convention in our work.

In section III, we shall review the factorization theorem in detail and extend it in the presence of the hadron mass. There are several different strategies to extract the FFs from data analysis. In the present analysis we adapt the zero-mass variable-flavor-number (ZM-VFN) scheme [34]. This scheme works best for high energy scales, where the heavy quark masses are set to zero from the start and the nonzero values of the c - and b -quark masses only enter through the initial conditions of the FFs. In

Table I: The individual χ^2 values at LO for each collaboration and the total χ^2 fit for proton.

collaboration	data properties	\sqrt{s} GeV	data points	$\chi^2(\text{LO})$ normalization in fit
TPC [28]	untagged	29	8	10.959
TASSO [29]	untagged	34	4	2.006
ALEPH [24]	untagged	91.2	18	18.211
SLD [27]	untagged	91.28	28	80.643
	<i>uds</i> tagged	91.28	29	61.263
	<i>c</i> tagged	91.28	29	40.286
	<i>b</i> tagged	91.28	28	60.358
DELPHI [25, 26]	untagged	91.2	17	2.990
	<i>uds</i> tagged	91.2	17	4.710
	<i>b</i> tagged	91.2	17	14.681
TOTAL: ($\chi^2/\text{d.o.f.}$)			195	296.107 1.711

Table II: As in Table I, but at NLO.

collaboration	data properties	\sqrt{s} GeV	data points	$\chi^2(\text{NLO})$ normalization in fit
TPC [28]	untagged	29	8	21.984
TASSO [29]	untagged	34	4	2.143
ALEPH [24]	untagged	91.2	18	19.955
SLD [27]	untagged	91.28	28	83.960
	<i>uds</i> tagged	91.28	29	43.920
	<i>c</i> tagged	91.28	29	39.010
	<i>b</i> tagged	91.28	28	45.795
DELPHI [25, 26]	untagged	91.2	17	4.734
	<i>uds</i> tagged	91.2	17	5.861
	<i>b</i> tagged	91.2	17	13.929
TOTAL: ($\chi^2/\text{d.o.f.}$)			195	281.291 1.626

this scheme, the number of active flavors also increases with the flavor thresholds.

B. Parametrization of proton FFs

In the phenomenological approach, the FFs are parametrized in a convenient functional form at an initial scale μ_0 at each order, i.e. LO and NLO, and then evolved to higher scales using the DGLAP evolution equations to fit to the existing experimental data. Various phenomenological models like Peterson model [10], Power model [38], Cascade model [39] etc., have been developed to describe the FFs. At the initial scale μ_0 , we apply the following flexible functional form for the proton FFs

$$D_i^p(z, \mu_0^2) = N_i z^{\alpha_i} (1-z)^{\beta_i} [1 - \delta_i e^{-\gamma_i z}], \quad (3)$$

which is an appropriate form for the light hadrons. Here, $z = x_p/x_i = E_p/E_i$ (with $i = g, u, \bar{u}, d, \bar{d}, \dots$) is the energy fraction of the parton i which is taken away by the produced proton. A simple polynomial parametrization with just three parameters controls the small- and large- z regions so that in (3), the power term in z restricts the small- z region and the power term in $(1-z)$ emphasizes the large- z region. To control the medium z -region and

to improve the accuracy of the global fit the extra term $[1 - \delta_i e^{-\gamma_i z}]$ is considered [17]. In order to get the best fit we assume $\delta_i = 1$ for light quarks and $\delta_i = 0$ for the gluon and heavy quark FFs. The free parameters N_i , α_i , β_i and γ_i in the proposed form are determined by minimizing χ^2 for differential cross section and experimental data $(1/\sigma_{tot} \cdot d\sigma^p/dx_p)_{exp}$. The χ^2 for k data points is defined as

$$\chi^2 = \sum_{j=1}^k \left(\frac{E_j - T_j}{\sigma_j^E} \right)^2. \quad (4)$$

Here, T_j and E_j stand for the theoretical results and experimental values of $1/\sigma_{tot} \times d\sigma^p/dx_p$, respectively. σ_j^E is the error of the corresponding experimental data including the statistical and systematical errors.

According to the partonic structure of the proton $p(uud)$ and the general functional form presented in (3), we consider the following forms for light-quark FFs

$$\begin{aligned} D_u^p(z, \mu_0^2) &= ND_d^p(z, \mu_0^2) = N_u z^{\alpha_u} (1-z)^{\beta_u} (1 - e^{-\gamma_u z}), \\ D_{\bar{u}}^p(z, \mu_0^2) &= N' D_{\bar{d}}^p(z, \mu_0^2) = N_{\bar{u}} z^{\alpha_{\bar{u}}} (1-z)^{\beta_{\bar{u}}} (1 - e^{-\gamma_{\bar{u}} z}), \\ D_s^p(z, \mu_0^2) &= D_{\bar{s}}^p(z, \mu_0^2) = N'' D_{\bar{u}}^p(z, \mu_0^2) \\ &= N_s z^{\alpha_{\bar{u}}} (1-z)^{\beta_{\bar{u}}} (1 - e^{-\gamma_{\bar{u}} z}), \end{aligned} \quad (5)$$

where the assumption $\delta_i = 1$ is used. For the gluon and heavy quark FFs, considering $\delta_i = 0$ we apply a power

Table III: Values of the fit parameters for the proton FFs at LO in the starting scales μ_0 .

flavor i	N_i	α_i	β_i	γ_i
u	0.028 ± 3.105	-1.547 ± 1.218	2.710 ± 0.657	0.052 ± 0.014
d	3.382 ± 1.185	-1.547 ± 1.218	2.710 ± 0.657	0.052 ± 0.014
\bar{u}	7.634 ± 1.481	-0.053 ± 0.021	5.389 ± 0.614	1.269 ± 0.618
\bar{d}	8.592 ± 3.268	-0.053 ± 0.021	5.389 ± 0.614	1.269 ± 0.618
s, \bar{s}	3.110 ± 2.009	-0.053 ± 0.021	5.389 ± 0.614	1.269 ± 0.618
c, \bar{c}	4.829 ± 2.700	0.733 ± 0.556	7.046 ± 2.093	...
b, \bar{b}	10.031 ± 3.430	0.681 ± 0.282	11.466 ± 1.360	...
g	1.237 ± 0.331	6.915 ± 2.380	0.482 ± 0.191	...

Table IV: As in Table III, but at NLO.

flavor i	N_i	α_i	β_i	γ_i
u	3.206 ± 2.852	-0.759 ± 0.179	17.935 ± 2.859	2.320 ± 0.225
d	3.284 ± 1.686	-0.759 ± 0.179	17.935 ± 2.859	2.320 ± 0.225
\bar{u}	21.005 ± 2.071	-0.533 ± 0.127	3.795 ± 1.281	0.1007 ± 0.035
\bar{d}	15.990 ± 2.352	-0.533 ± 0.127	3.795 ± 1.281	0.1007 ± 0.035
s, \bar{s}	7.999 ± 1.580	-0.533 ± 0.127	3.795 ± 1.281	0.1007 ± 0.035
c, \bar{c}	6.120 ± 1.575	0.826 ± 0.217	7.949 ± 1.957	...
b, \bar{b}	7.218 ± 1.605	0.560 ± 0.108	11.617 ± 2.307	...
g	3.739 ± 1.862	4.290 ± 0.814	1.736 ± 0.218	...

model in our calculations, as applied by DSS [22] and HKNS [23] collaborations, i.e.

$$\begin{aligned}
D_g^p(z, \mu_0^2) &= N_g z^{\alpha_g} (1-z)^{\beta_g}, \\
D_c^p(z, \mu_0^2) &= D_{\bar{c}}^p(z, \mu_0^2) = N_c z^{\alpha_c} (1-z)^{\beta_c}, \\
D_b^p(z, \mu_0^2) &= D_{\bar{b}}^p(z, \mu_0^2) = N_b z^{\alpha_b} (1-z)^{\beta_b}. \quad (6)
\end{aligned}$$

The assumption $\delta_i = 0$ in (3) for the gluon and heavy quark FFs makes a more convenient fit by reducing the minimized χ^2 -values. In the equations above, we also considered the isospin symmetry for sea quarks of proton FFs. Considering Eqs. (5) and (6), there are 20 parameters which must be determined by fitting. In the reported parameters by AKK [16] and HKNS [23] some parameters such as N and N' (5) are fixed from the beginning, i.e. a simple parameterization form is applied.

In our parametrization, the starting scale μ_0 is different for various partons. The value of $\mu_0^2 = 1 \text{ GeV}^2$ is chosen for the splitting of a gluon and light-quarks into the proton and for the c - and b -quarks it is taken to be $\mu_0^2 = m_c^2$ and $\mu_0^2 = m_b^2$, respectively.

According to the partonic structure of the proton, the proton FFs can be applied for the anti-proton as

$$D_i^{\bar{p}}(z, \mu_0^2) = D_i^p(z, \mu_0^2). \quad (7)$$

C. Experimental data and our analysis

In our fits of the proton FFs, we consider SIA data from LEP (*ALEPH* [24] and *DELPHI* [25, 26] collaborations), SLAC (*SLD* [27] and *TPC* [28] collaborations) and DESY (*TASSO* [29] collaboration). The energy scales of the experimental data range from 29 GeV to 91.28 GeV.

Most of the precision e^+e^- annihilation data, however, come from the LEP and SLAC data at the energy scale of $Q^2 = M_Z^2$. In the data sets reported by the *DELPHI* and *SLD*, authors distinguished between four cases: fragmentation of u , d and s quarks, c quarks only, b quarks only, and all five quark flavors (see Tables I and II).

Note that in our global analysis of data sets from the *ALEPH* experiments we deal with data in the form of $1/N \times dN^p/dx_p$, where N is the number of detected events. This fraction is defined as the ratio of the single-inclusive e^+e^- annihilation cross section ($e^+e^- \rightarrow p+X$) in a certain bin of x_p to the totally inclusive rate, i.e. $1/\sigma_{tot} \times d\sigma^p/dx_p$, where x_p refers to the energy of proton scaled to the beam energy \sqrt{s} , i.e. $x_p = 2E_p/\sqrt{s}$.

In Tables I and II, based on each collaboration the data characteristics, the χ^2 (4) and the χ^2 values per degree of freedom ($\chi^2/d.o.f$) are listed. The obtained values of $\chi^2/d.o.f$ for the proton at LO and NLO are 1.711 and 1.626 in our global fit, respectively. In section III, we will show that this value is reduced when one includes the effects of the proton mass in the calculations.

Our LO and NLO results for the fit parameters in the starting scales μ_0^2 along with the corresponding uncertainties are listed in Tables III and IV. The method of error calculation shall be described in next subsection.

In Fig. 1, using the NLO results for the proton FFs (Table IV) and applying the DGLAP equations, we compare our results for $1/\sigma_{tot} \times d\sigma^p/dx_p$ with SIA experimental data at $\mu^2 = M_Z^2$ reported by the *ALEPH* [24], *DELPHI* [25, 26] and *SLD* [27] collaborations. In these figures we separate the light, charm and bottom tagged cross sections, and as it is seen most of the diagrams are in a reliable consistency with the experimental data. Note that, as Fig. 1 shows, due to the largeness of the χ^2 con-

tribution for the SLD b-tagged data (see Table. II) some points are outside of the curves. However, χ^2 -values of the heavy quarks are usually larger than the other data and this might be caused to some extent by contaminations from weak decay.

The NLO proton FFs are presented in Fig. 2 at their corresponding initial scales; $\mu_0^2 = 1 \text{ GeV}^2$ for the gluon and light quarks, $\mu_0^2 = m_c^2$ and $\mu_0^2 = m_b^2$ for the c - and b -quarks, respectively. In Fig. 3, our results for the fragmentation densities are presented at the scales $Q^2 = 2 \text{ GeV}^2$ for the gluon and light quarks, and $Q^2 = 4 \text{ GeV}^2$ and $Q^2 = 25 \text{ GeV}^2$ for the c - and b -quarks, respectively. Our results for different flavors are compared with the DSS set of proton FFs [22] that included electron-positron, lepton-nucleon, and hadron-hadron scattering data, and the HKNS FFs [23] that included electron-positron data. For more comparison we have also applied the AKK extraction of proton FFs at NLO [16] that included hadron production data in electron-positron and hadron-hadron scattering data. Comparing our model with other FF models gives a nice all-around description of our model. As is seen, our results for the heavy quark FFs are in a reliable consistency with the results obtained by HKNS collaboration. In this figure, considering the proton mass effects we also show the massive FFs (solid line) and their error bands at NLO, a topic which is explained in section III.

D. The Gaussian method to calculate errors

According to (5) and (6), the evolved proton FFs are attributive functions of the input parameters which are calculated from the fit, and their standard linear errors are given by Gaussian error propagation. If $D_i^H(z, Q^2)$ is the evolved fragmentation density at the scale Q^2 , then the Gaussian error propagation is defined as

$$[\delta D_i^H(z)]^2 = \Delta\chi^2 \sum_{j,k}^n \frac{\partial D_i^H(z, a_j)}{\partial a_j} (H_{jk})^{-1} \frac{\partial D_i^H(z, a_k)}{\partial a_k}, \quad (8)$$

where $\Delta\chi^2$ is the allowed variation in χ^2 , $a_j |_{j=1}^n$ are fit parameters and n is the number of parameters in the global fit. H_{jk} are the elements of the Hessian or covariance matrix of the parameters determined in the QCD analysis at the initial scale Q_0^2 which are defined as

$$H_{jk} = \frac{1}{2} \frac{\partial^2 \chi^2}{\partial a_j \partial a_k} \Big|_{\min}. \quad (9)$$

Consequently, we can calculate the uncertainties of any FFs by using the Hessian matrix based on the Gaussian method at any value of Q^2 by the QCD evolution. The results indicate that the FFs, especially gluon and light-quark FFs, have large uncertainties at small Q^2 . More information and a detailed discussion can be found in [18, 23].

III. PROTON MASS EFFECTS

In this section, we show how to incorporate the hadron mass effects into inclusive hadron production in e^+e^- reaction and into its relevant kinematic variables. The same scheme can be applied for hadron-hadron reactions. To explain our procedure, at first, we review the factorization theorem and its kinematic variables defined. Consider the following process

$$e^+e^- \rightarrow \gamma/Z(q) \rightarrow i(p_i)\bar{i}(p_{\bar{i}}) \rightarrow H(p_H) + X, \quad (10)$$

where the four-momenta of particles are shown in the parenthesis, and $s = q^2$ is the squared of the center-of-mass (c.m.) energy. By ignoring the mass of produced hadron H and outgoing partons i and \bar{i} , in the c.m. frame the momenta take the following form

$$q = (\sqrt{s}, \vec{0}), \quad p_i = (E_i, \vec{0}, E_i), \quad p_H = (E_H, \vec{0}, E_H), \quad (11)$$

where we assumed that the parent partons, i.e. i and \bar{i} , and produced hadron are emitted in the direction of the 3-axis. Considering the definition of the cross section, one can write

$$d\sigma(x_H, s) = \sum_{i=u,d,s,\dots} \int dz d\hat{\sigma}_i(\mu_R^2, \mu_F^2) \Big|_{E_i=E_H/z} D_i^H(z, \mu_F^2), \quad (12)$$

where $d\hat{\sigma}_i$ are the Wilson coefficients in the parton level (the cross sections for the processes $e^+e^- \rightarrow i\bar{i}$) and D_i^H is the $i \rightarrow H$ FF. Here, $x_H = 2p_H \cdot q / q^2 = 2E_H / \sqrt{s}$ and $z = E_H / E_i$ are the scaling variables. Since the measured observable is $d\sigma/dx_H$, by defining $x_i = 2p_i \cdot q / q^2 = 2E_i / \sqrt{s}$ one can write $d\hat{\sigma}_i = dx_H (dx_i/dx_H) d\hat{\sigma}_i/dx_i$, then

$$\frac{d\sigma}{dx_H}(x_H, s) = \sum_i \int dz \frac{d\hat{\sigma}_i}{dx_i} \frac{dx_i}{dx_H} D_i^H\left(\frac{x_H}{x_i}, \mu_F^2\right). \quad (13)$$

Considering the definition $x_i = x_H/z$, one has $dx_i/dx_H = 1/z$ and, therefore, one can write $dz/z = -dx_i/x_i$ so that the equation above is simplified to the following form

$$\frac{d\sigma}{dx_H}(x_H, s) = \sum_i \int_{x_H}^1 \frac{dx_i}{x_i} \frac{d\hat{\sigma}_i}{dx_i} D_i^H\left(\frac{x_H}{x_i}, \mu_F^2\right), \quad (14)$$

that leads to the relation (2). In the equation above, one has $\sqrt{\rho_H^2} \leq x_H \leq 1$ where $\rho_H = 2m_H/\sqrt{s}$ is the cut-off and if one sets the hadron mass as $m_H = 0$, then $0 \leq x_H \leq 1$.

Note that, to establish the factorization theorem we ignored the hadron and parton masses when we defined the scaling variables x_H and x_i . To incorporate the hadron mass effects we use a specific choice of scaling variables. For this purpose, it would be helpful to work with light-cone (L.C) coordinates, in which any four-vector V is written in the form of $V = (V^+, V^-, \vec{V}_T)$

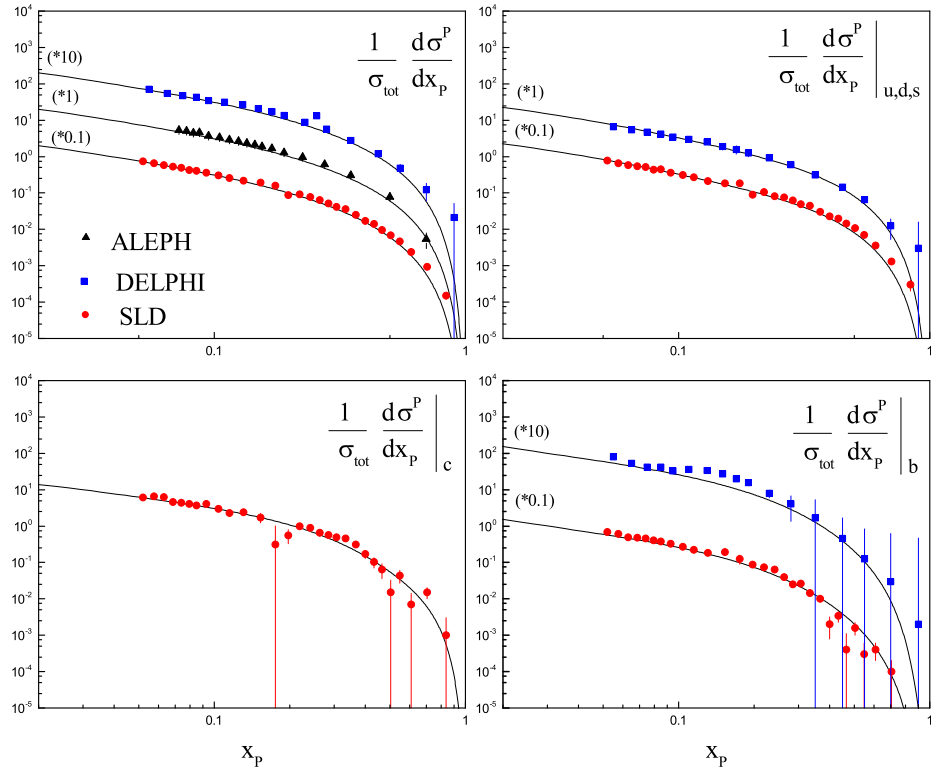


Figure 1: Comparison of our NLO results for $1/\sigma_{\text{tot}} \times d\sigma/dx_p$ in total and tagged cross sections with proton production data at $Q^2 = M_Z^2$ by *ALEPH* [24], *DELPHI* [25, 26] and *SLD* [27].

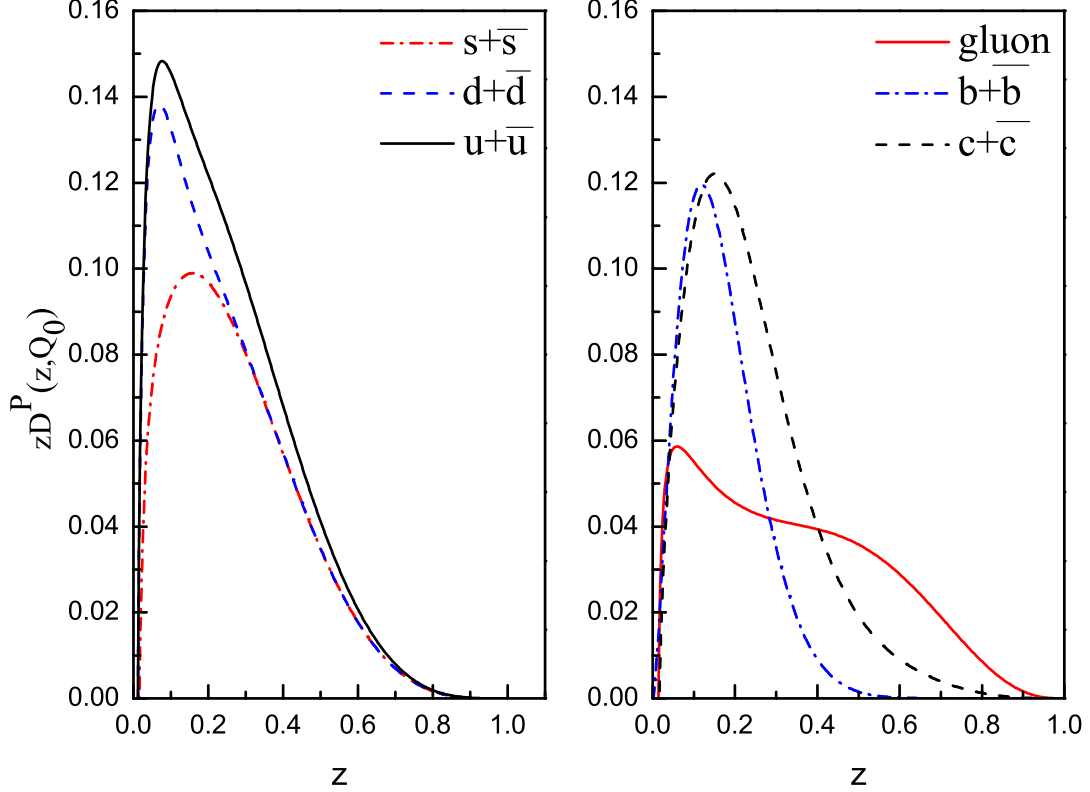


Figure 2: Proton fragmentation functions are shown at $Q_0^2 = 1 \text{ GeV}^2$, m_c^2 and m_b^2 at NLO.

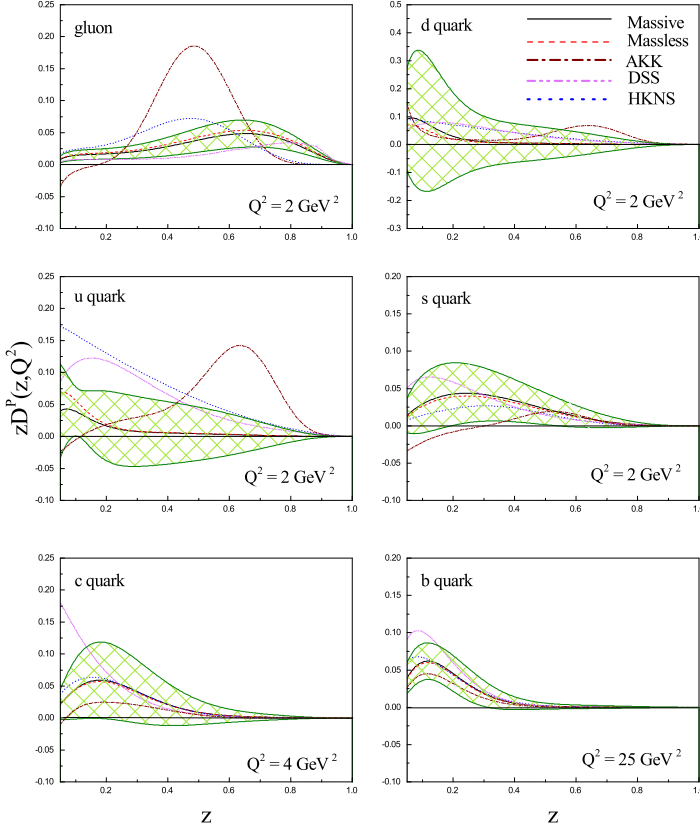


Figure 3: The NLO fragmentation densities for the massless (dashed line) and massive (solid line) protons are shown at $Q^2 = 2 \text{ GeV}^2$, 4 GeV^2 and 25 GeV^2 for the gluon and light quarks, the c - and b -quarks, respectively. The uncertainties of massive proton FFs are also shown. Our results are compared with AKK [16], DSS [22] and HKNS [23] collaborations.

with $V^\pm = (V^0 \pm V^3)/\sqrt{2}$ and $\vec{V}_T = (V^1, V^2)$. Considering the L.C coordinates, the four-momenta of particles in the e^+e^- reaction (11) are expressed as

$$q = \left(\frac{\sqrt{s}}{\sqrt{2}}, \frac{\sqrt{s}}{\sqrt{2}}, \vec{0}\right), \quad p_H = (\sqrt{2}E_H, 0, \vec{0}), \quad (15)$$

and $p_i = (\sqrt{2}E_i, 0, \vec{0})$. Therefore, in absence of the hadron mass, the scaling variable $x_H = 2E_H/\sqrt{s}$ is expressed as $x_H = p_H^+/q^+$ in the L.C coordinates. From now on, in the presence of hadron mass, we define a new variable $\eta = p_H^+/q^+$ as a light-cone scaling variable which is identical to the x_H -variable in the absence of a hadron mass. The variable η is now a more convenient scaling variable for studying hadron mass effects, because it is invariant with respect to boosts along the direction of the hadron's spatial momentum (Z -axis). Taking a mass m_H for the hadron, the momentum of the hadron in the c.m. frame reads

$$p_H = (p_H^+, p_H^-, \vec{p}_T) = (\eta q^+, p_H^-, \vec{p}_T) = \left(\eta \frac{\sqrt{s}}{\sqrt{2}}, p_H^-, \vec{0}\right). \quad (16)$$

With respect to $p_H^2 = m_H^2$ and considering the inner product in the L.C system ($V \cdot V = 2V^+V^- - V_T^2$), the hadron momentum is expressed as

$$p_H = \left(\eta \frac{\sqrt{s}}{\sqrt{2}}, \frac{m_H^2}{\eta\sqrt{2}s}, \vec{0}\right). \quad (17)$$

As a generalization of the massless case, the cross section in the new coordinates is obtained by the replacements $x_H \rightarrow \eta (= p_H^+/q^+)$ and $x_i \rightarrow y (= p_i^+/q^+)$ in (14), i.e.

$$\frac{d\sigma}{d\eta}(\eta, s) = \sum_i \int_\eta^1 \frac{dy}{y} \frac{d\hat{\sigma}}{dy} D_i^H\left(\frac{\eta}{y}, \mu_F\right). \quad (18)$$

Since the experimental quantity is $d\sigma/dx_H$, it can be related to $d\sigma/d\eta$ via

$$\frac{d\sigma}{dx_H}(x_H, s) = \frac{d\sigma}{d\eta}(\eta, s) \times \frac{d\eta}{dx_H}. \quad (19)$$

By comparing the hadron momentum in the L.C system, $p_H = ((p_H^0 + p_H^3)/\sqrt{2}, (p_H^0 - p_H^3)/\sqrt{2}, \vec{0})$, with the equation (17), the equality relation between two scaling variables results

$$p_H^0 = \frac{1}{2}(\eta\sqrt{s} + \frac{m_H^2}{\eta\sqrt{s}}) \Rightarrow x_H = \eta(1 + \frac{m_H^2}{s\eta^2}). \quad (20)$$

Note that, these two variables are approximately equal when $m_h \ll x_H\sqrt{s}$. Considering equation (20), one has

$$\frac{d\eta}{dx_H} = \frac{1}{1 - \frac{m_H^2}{s\eta^2(x_H)}}. \quad (21)$$

Finally, the differential cross section in the presence of hadron mass reads

$$\frac{d\sigma}{dx_H}(x_H, s) = \frac{1}{1 - \frac{m_H^2}{s\eta^2(x_H)}} \frac{d\sigma}{d\eta}(\eta(x_H), s). \quad (22)$$

The above formula, established for the first time, would be a fundamental relation for the factorization theorem extended in the presence of hadron mass and it would be more effective and applicable when the hadron mass is considerable (especially, larger than the proton mass). Among all well-known collaborations, the only collaboration who studied the effects of proton mass into their calculations is AKK collaboration [16]. The AKK have used the same coordinates to include the effects of hadron mass in their analysis. Due to the data used in their analysis, they have identified the scaling variable $x_m = 2|\vec{p}|/\sqrt{s}$, where $|\vec{p}|$ stands for the three-momentum of the produced hadron, while in our analysis we use the energy scaling variable $x_H = 2E_H/\sqrt{s}$. Therefore, the differential cross section (or the extended factorization formula), including the hadron mass effects computed in our work, is different with the one ($d\sigma/dx_m$) presented in [16]. The effect of hadron mass is to reduce the size of the cross section $d\sigma/dx_m$ at small x_m , while this effect increases the

cross section $d\sigma/dx_H$ at small x_H . Besides, as was mentioned, the AKK has applied a simple parameterization form for the proton FFs by fixing some free parameters from the beginning and they have also not determined the uncertainties of the proton FFs.

In Table. V, we list all experimental data sets included in our global analysis, and the χ^2 value per degree of freedom pertaining to the NLO fit including the proton mass effects. As is seen, the inclusion of the proton mass leads to a reduction of the value of $\chi^2/d.o.f$, which is now 1.583 in our global fit. Our results for the fit parameters, in the presence of the proton mass, are listed in Table. VI. Using the Gaussian method, their uncertainties are also shown. In Fig. 3, using the fit parameters presented in Table. VI, the massive proton FFs (solid line) are shown at the scales $Q^2 = 2 \text{ GeV}^2$, 4 GeV^2 and 25 GeV^2 for the gluon and light quarks, the c - and b -quarks, respectively. Considering errors presented in Table. VI, the uncertainties of the massive proton FFs are also shown. In Figs. 4 and 5, the effect of proton mass on the parton FFs are shown at the scales $Q = 29 \text{ GeV}$ and $Q = 34 \text{ GeV}$, respectively. The massless (dotted line) and massive (solid line) FFs are also compared with the results obtained by AKK collaboration [16], who used the proton mass effects too. As it is seen, the mass of the proton affects the FFs of the gluon and light quarks d and u . It is also seen that our results for the gluon, d - and u -quark FFs deviate from the AKK extractions of FFs; however the data sets and the extended factorization theorem in their analysis are different. In Fig. 6, our results for $1/\sigma_{tot} \times d\sigma^p/dx_p$ in the presence of massless and massive protons are compared with the data from the TPC collaboration at $Q = 29 \text{ GeV}$. In Fig. 7, the same comparison is done with the data from the TASSO collaboration at $Q = 34 \text{ GeV}$. Note that the effect of the proton mass is that it reduces the size of the differential cross section at large x_p . This is needed to improve the fit when one works with data from TPC. As is shown, the effect of the proton mass is that it increases the size of the cross section at small x_p so that improves the fit when we work with the data from the TASSO collaboration, see Fig. 7.

Table V: The individual χ^2 values for each collaboration and the total χ^2 fit for proton when including the proton mass.

collaboration	data properties	$\sqrt{s} \text{ GeV}$	data points	$\chi^2(\text{NLO})$ normalization in fit
TPC [28]	untagged	29	8	20.648
TASSO [29]	untagged	34	4	2.118
ALEPH [24]	untagged	91.2	18	18.408
SLD [27]	untagged	91.28	28	83.724
	uds tagged	91.28	29	42.743
	c tagged	91.28	29	38.603
	b tagged	91.28	28	43.927
DELPHI [25, 26]	untagged	91.2	17	4.390
	uds tagged	91.2	17	4.994
	b tagged	91.2	17	14.241
TOTAL:			195	273.796
$(\chi^2/d.o.f)$				1.583

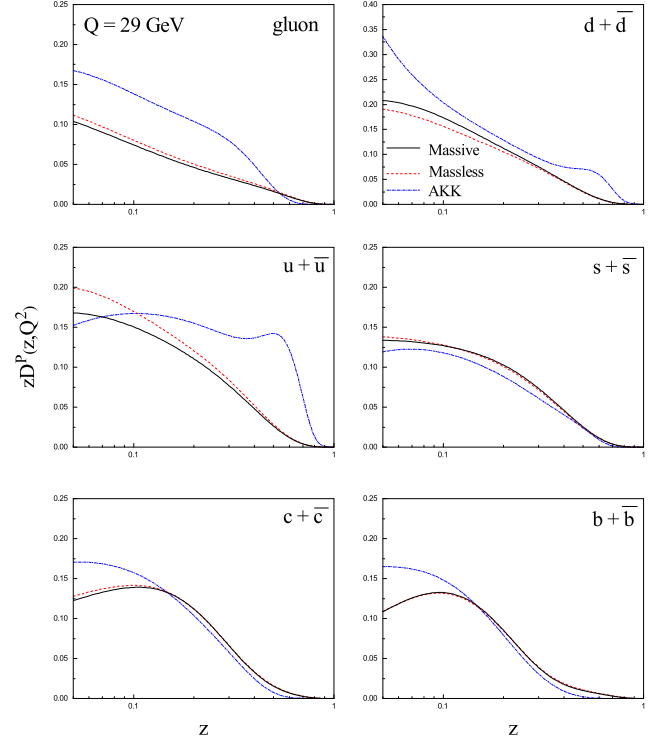


Figure 4: Comparison of the NLO proton FFs at $Q = 29 \text{ GeV}$ for massive (solid lines) and massless (dotted lines) protons. The results are also compared with AKK [16] collaboration.

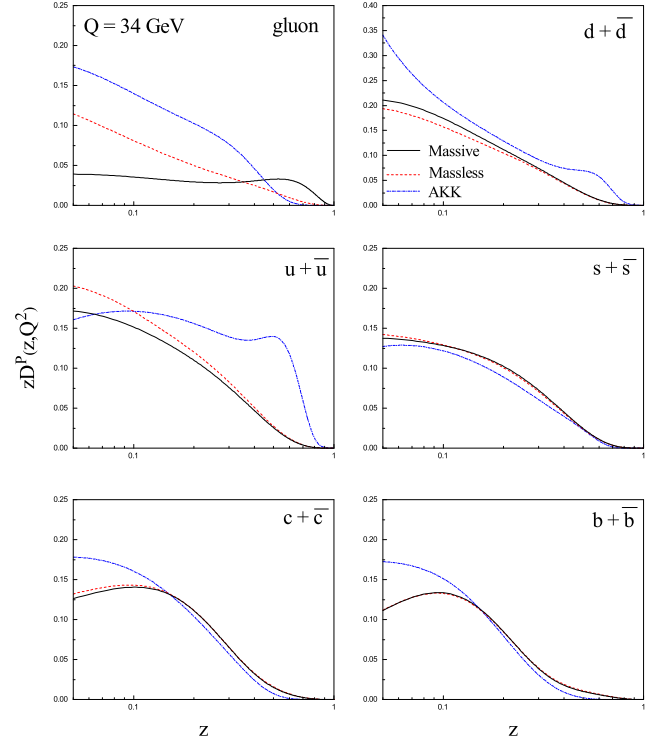


Figure 5: As in Fig. 4, but at $Q = 34 \text{ GeV}$.

Table VI: Values of the fit parameters for the proton FFs at NLO, by including proton mass effects in the fit. We set the proton mass as $m_p = 938.272$ MeV.

flavor i	N_i	α_i	β_i	γ_i
u	2.016 ± 2.189	-0.695 ± 0.165	16.080 ± 2.329	2.314 ± 0.152
d	4.676 ± 1.879	-0.695 ± 0.165	16.080 ± 2.329	2.314 ± 0.152
\bar{u}	19.005 ± 2.002	-0.601 ± 0.070	3.665 ± 1.106	0.090 ± 0.017
\bar{d}	17.984 ± 3.707	-0.601 ± 0.070	3.665 ± 1.106	0.090 ± 0.017
s, \bar{s}	8.878 ± 1.809	-0.601 ± 0.070	3.665 ± 1.106	0.090 ± 0.017
c, \bar{c}	6.908 ± 2.042	0.867 ± 0.137	7.967 ± 2.069	...
b, \bar{b}	7.560 ± 2.176	0.569 ± 0.169	11.569 ± 1.284	...
g	3.515 ± 1.154	4.388 ± 0.433	1.739 ± 0.117	...

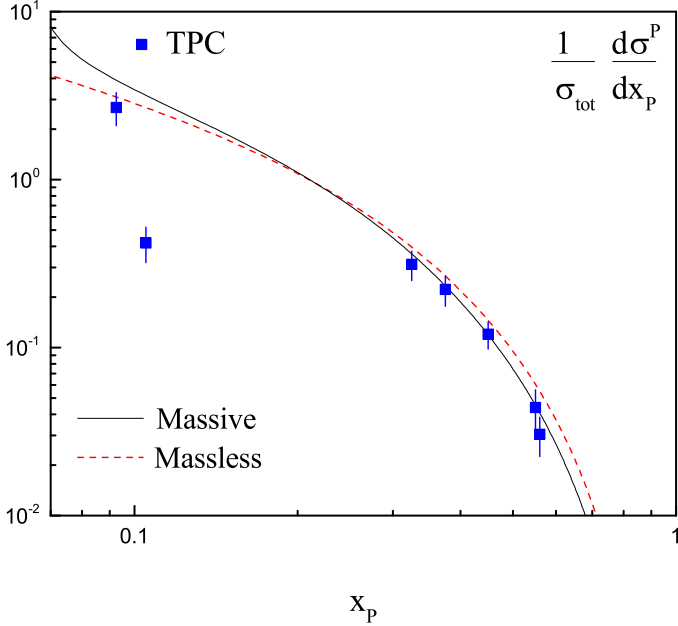


Figure 6: Comparison of our NLO results for the total cross section $1/\sigma_{tot} \times d\sigma/dx_p$ with data from *TPC* [28] at $Q = 29$ GeV. The effect of proton mass is also considered in the solid curve.

IV. ENERGY SPECTRUM OF THE INCLUSIVE PROTON IN TOP QUARK DECAYS

In this section, we apply the massive proton FFs to make phenomenological predictions for the energy spectrum of protons produced in unpolarized top decays

$$t \rightarrow b + W^+(g) \rightarrow p + X, \quad (23)$$

where X stands for the unobserved final state. Both the b -quark and the gluon may hadronize into the produced protons, while the gluon contributes to the real radiation at NLO.

Generally, to obtain the energy distribution of the produced hadron H , we employ the factorization theorem

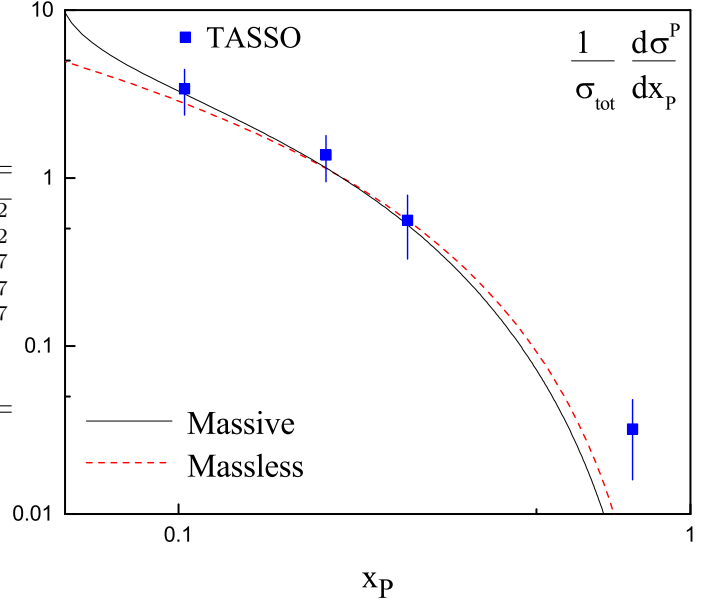


Figure 7: As in Fig. 6, but comparison is done with data from *TASSO* [29] at $Q = 34$ GeV.

(14), which is now expressed as

$$\frac{d\Gamma}{dx_H} = \sum_{i=b,g} \int_{x_i^{min}}^{x_i^{max}} \frac{dx_i}{x_i} \frac{d\hat{\Gamma}}{dx_i}(\mu_R, \mu_F) D_i^H\left(\frac{x_H}{x_i}, \mu_F\right), \quad (24)$$

where, as in [4], we defined the scaled-energy fraction of the hadron as $x_H = 2E_H/(m_t^2 - m_W^2)$ and $d\hat{\Gamma}/dx_i$ are the parton-level differential decay rates of the process $t \rightarrow i + W^+(i = b, g)$. The NLO analytical expressions for the parton-level differential decay widths $d\hat{\Gamma}/dx_i$ are presented in Refs. [3, 4]. In [40], we studied the effects of parton and hadron masses on the hadron energy spectrum produced through top decays.

In (24), the factorization and the renormalization scales are set to $\mu_R = \mu_F = m_t = 172.9$ GeV and we also set $m_b = 4.78$ GeV, $\Lambda^{NLO} = 231$ MeV and $m_W = 80.39$ GeV.

In Fig. 8, to show our prediction for the energy spectrum of produced protons we study the size of the NLO corrections, by showing the total result (solid line), and comparing the relative importance of the $b \rightarrow p$ (dashed line) and $g \rightarrow p$ (dot-dashed line) fragmentation channels. As is seen, the gluon contribution (dot-dashed line) is negative and appreciable only in the low x_p region. For higher values of x_p ($x_p > 0.3$) the NLO result is practically exhausted by the $b \rightarrow p$ contribution, as expected [4]. Note that the contribution of the gluon FF cannot be discriminated. It is calculated to see where it contributes to $d\Gamma/dx_p$. So, this part of the plot is of more theoretical relevance. In the scaled-energy of hadrons, as an experimental quantity, all contributions including the b -quark and gluon contribute. In Fig. 9, our prediction for $d\Gamma(t \rightarrow p + X)/dx_p$ is compared with the result

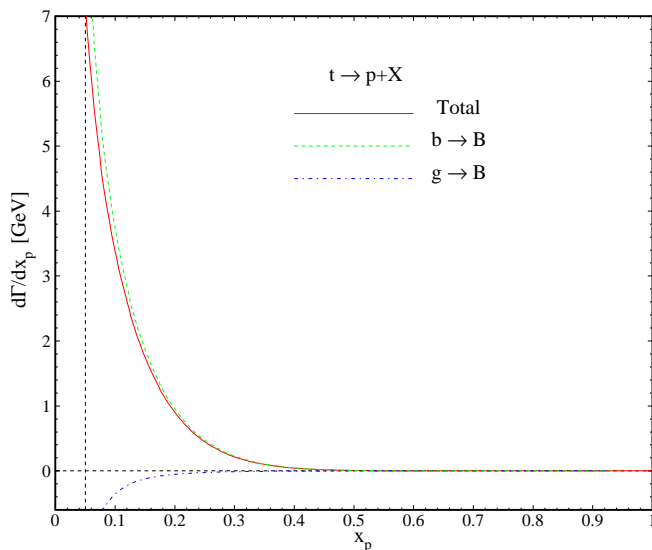


Figure 8: $d\Gamma(t \rightarrow p+X)/dx_p$ as a function of x_p (solid line) at $\mu_F = m_t$. The NLO result is broken up into the contributions due to $b \rightarrow p$ (dashed line) and $g \rightarrow p$ (dot-dashed line) fragmentations.

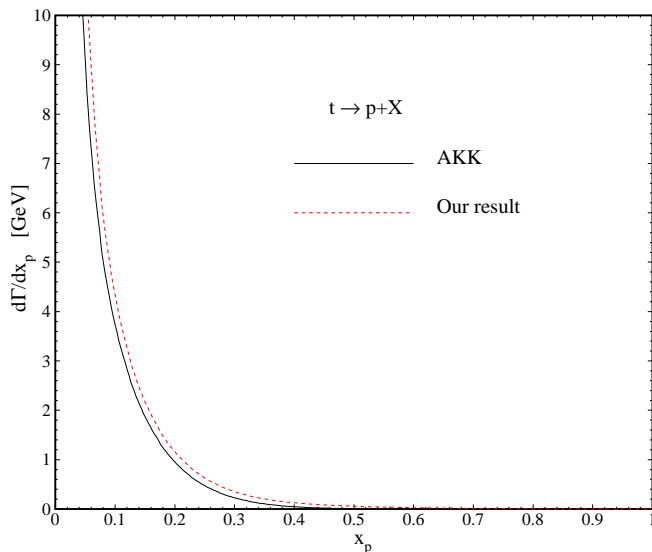


Figure 9: Result for the partial decay rate $d\Gamma/dx_p$ is shown using the extracted $(b, g) \rightarrow p$ FFs in the presence of the proton mass. We also show the same distribution using the FFs presented by AKK [16].

obtained by using the FFs extracted by the AKK collaboration [16]. Considering Figs. 4 and 5, it is seen that our results for the b-quark fragmentation function are in good consistency with the results extracted by the AKK for the values higher than $z \geq 0.1$, then one expects to have the same results for the $d\Gamma/dx_p$ in both analysis.

V. CONCLUSION

We determined new nonperturbative fragmentation functions for the proton in the parton model of QCD

through a global analysis on SIA data at the LO and NLO approximations. Our new parametrization of the proton FFs covers a wide kinematic range of z , in the presence of the extra term $(1 - \delta_i e^{-\gamma_i z})$ which controls the medium- z region and improves the accuracy of the global fit. Fig. 1 represents the comparison of our model with SIA experimental data and shows that our model is successful. We determined the FFs of gluon and light quarks at the initial scale $\mu_0^2 = 1 \text{ GeV}^2$ and the FFs of heavy quarks at $\mu_0^2 = m_c^2$ and $\mu_0^2 = m_b^2$. Their evaluation was performed by using the DGLAP equations. Our analysis was based on the ZM-VFN scheme, where all partons are treated as massless particles and the nonzero values of the c- and b-quark masses only enter through the initial conditions of the FFs. Comparing to other collaborations we also considered the effects of the proton mass on the FFs and showed that this effect improves the accuracy of the global fit, specifically for the data from SLAC (TPC collaborations) and DESY (TASSO collaboration). The proton mass affects the light and gluon FFs while for the heavy quark FFs this effect is less important. The advent of precise data from LHC offers us the opportunity to further constrain the proton FFs and to test their scaling violations. This situation motivates the incorporation of proton mass effects into the formalism, which are then likely to be no longer negligible. The mass of the proton also sets a bound on the scaling variable $x_p \geq 2m_p/\sqrt{s}$.

Finally, as an application, we used the computed FFs to study the scaled-energy distribution of protons in unpolarized top quark decays. At LHC, the scaled-energy distribution of hadrons in top decays enables us to deepen our knowledge of the hadronization process. The universality and scaling violations of the proton FFs will be able to be tested at the LHC by comparing our NLO predictions with future measurements of $d\Gamma/dx_p$.

Besides NLO corrections, some other corrections can improve our analysis. In future work, we plan to extend the method developed in [41] in the framework of e^+e^- annihilation to resum large logarithmic terms, due to soft-gluon radiation, to all perturbative orders in the QCD coupling α_s .

Acknowledgments

We are grateful to Gennaro Corcella for his careful reading of the manuscript and also for constructive discussions and comments. We would also like to thank Mathias Butenschon for reading and editing the English manuscript and Bernd A. Kniehl and the DESY theoretical division for their hospitality, where a portion of this work was performed.

-
- [1] D. P. Anderle, F. Ringer and M. Stratmann, Phys. Rev. D **92** (2015) no.11, 114017.
 - [2] S. M. M. Nejad, Phys. Rev. D **88**, no. 9, 094011 (2013).
 - [3] B. A. Kniehl, G. Kramer and S. M. Moosavi Nejad, Nucl. Phys. B **862** (2012) 720.
 - [4] G. Corcella and A. D. Mitov, Nucl. Phys. B **623**, 247 (2002).
 - [5] CMS Collaboration [CMS Collaboration], CMS-PAS-TOP-15-002.
 - [6] G. Corcella, arXiv:1511.08429 [hep-ph].
 - [7] J. P. Ma, Nucl. Phys. B **506** (1997) 329.
 - [8] E. Braaten and T. C. Yuan, Phys. Rev. Lett. **71** (1993) 1673.
 - [9] J. D. Bjorken, Phys. Rev. D **17** (1978) 171.
 - [10] C. Peterson, D. Schlatter, I. Schmitt and P. M. Zerwas, Phys. Rev. D **27** (1983) 105.
 - [11] M. Suzuki, Phys. Lett. B **71** (1977) 139.
 - [12] F. Amiri and C. -R. Ji, Phys. Lett. B **195** (1987) 593.
 - [13] S. M. M. Nejad and A. Armat, Eur. Phys. J. Plus **128** (2013) 121.
 - [14] S. M. Moosavi Nejad, Eur. Phys. J. Plus **130** (2015) 7, 136.
 - [15] F. Arbabifar, A. N. Khorramian and M. Soleymaninia, Phys. Rev. D **89**, no. 3, 034006 (2014).
 - [16] S. Albino, B. A. Kniehl and G. Kramer, Nucl. Phys. B **803**, 42 (2008); S. Albino, B. A. Kniehl and G. Kramer, Nucl. Phys. B **725** (2005) 181; S. Albino, B. A. Kniehl, G. Kramer and W. Ochs, Phys. Rev. D **73**, 054020 (2006).
 - [17] M. Soleymaninia, A. N. Khorramian, S. M. Moosavi Nejad and F. Arbabifar, Phys. Rev. D **88**, no. 5, 054019 (2013) [Phys. Rev. D **89**, no. 3, 039901 (2014)].
 - [18] M. Soleymaninia, A. N. Khorramian, S. M. Moosavi Nejad and F. Arbabifar, Acta Phys. Polon. Supp. **7**, no. 3, 573 (2014).
 - [19] E. Leader, A. V. Sidorov and D. B. Stamenov, arXiv:1506.06381 [hep-ph].
 - [20] D. de Florian, R. Sassot, M. Epele, R. J. Hernandez-Pinto and M. Stratmann, Phys. Rev. D **91** (2015) 1, 014035.
 - [21] D. de Florian, R. Sassot and M. Stratmann, Phys. Rev. D **75**, 114010 (2007).
 - [22] D. de Florian, R. Sassot and M. Stratmann, Phys. Rev. D **76**, 074033 (2007).
 - [23] M. Hirai, S. Kumano, T. -H. Nagai and K. Sudoh, Phys. Rev. D **75**, 094009 (2007).
 - [24] D. Buskulic *et al.* (ALEPH collaboration), Z. Phys. **C66**, 355 (1995); R. Barate *et al.*, Phys. Rep. **294**, 1 (1998).
 - [25] P. Abreu *et al.* (DELPHI collaboration), Eur. Phys. J. **C5**, 585 (1998).
 - [26] P. Abreu *et al.* (DELPHI collaboration), Nucl. Phys. **B444**, 3 (1995).
 - [27] K. Abe *et al.* (SLD collaboration), Phys. Rev. **D69**, 072003 (2004).
 - [28] H. Aihara *et al.* (TPC collaboration), Phys. Rev. Lett. **52**, 577 (1984); **61**, 1263 (1988).
 - [29] W. Braunschweig *et al.* (TASSO collaboration), Z. Phys. **C42**, 189 (1989).
 - [30] K. G. Chetyrkin, R. Harlander, T. Seidensticker and M. Steinhauser, Phys. Rev. D **60** (1999) 114015.
 - [31] J. C. Collins, Phys. Rev. D **58** (1998) 094002.
 - [32] J. C. Collins and D. E. Soper, Ann. Rev. Nucl. Part. Sci. **37** (1987) 383.
 - [33] V. N. Gribov and L. N. Lipatov, Sov. J. Nucl. Phys. **15**, 438 (1972) [Yad. Fiz. **15**, 781 (1972)]; G. Altarelli and G. Parisi, Nucl. Phys. **B126**, 298 (1977); Yu. L. Dokshitzer, Sov. Phys. JETP **46**, 641 (1977) [Zh. Eksp. Teor. Fiz. **73**, 1216 (1977)].
 - [34] T. Kneesch, B. A. Kniehl, G. Kramer and I. Schienbein, Nucl. Phys. B **799**, 34 (2008).
 - [35] S. Kretzer, Phys. Rev. D **62**, 054001 (2000).
 - [36] B. A. Kniehl and G. Kramer, Phys. Rev. D **71**, 094013 (2005).
 - [37] J. Binnewies, B. A. Kniehl and G. Kramer, Z. Phys. C **65**, 471 (1995).
 - [38] B. A. Kniehl, G. Kramer, I. Schienbein and H. Spiesberger, Phys. Rev. D **77**, 014011 (2008).
 - [39] B. R. Webber, Nucl. Phys. B **238** (1984) 492.
 - [40] S. M. Moosavi Nejad and M. Balali, arXiv:1602.05322 [hep-ph].
 - [41] M. Cacciari and S. Catani, Nucl. Phys. B **617** (2001) 253.